Optically Implemented Broadband Blueshift Switch in the Terahertz Regime

Nian-Hai Shen, Maria Massaouti, Mutlu Gokkavas, Jean-Michel Manceau, Ekmel Ozbay, Maria Kafesaki, Thomas Koschny, Stelios Tzortzakis, and Costas M. Soukoulis

Phys. Rev. Lett. **106**, 037403 — Published 18 January 2011

DOI: 10.1103/PhysRevLett.106.037403

Optically implemented broadband blue-shift switch in the terahertz regime

Nian-Hai Shen,[1] Maria Massaouti,[2] Mutlu Gokkavas,[3] Jean-Michel Manceau,[2] Ekmel Ozbay,[3] Maria Kafesaki,[2,4] Thomas Koschny,[1,2] Stelios Tzortzakis,[2,*] and Costas M. Soukoulis[1,2,4,†]

[1] *Ames Laboratory and Department of Physics and Astronomy, Iowa State University, Ames, Iowa 50011, U.S.A.*
[2] *Institute of Electronic Structure and Laser, FORTH, 71110 Heraklion, Crete, Greece*
[3] *Nanotechnology Research Center, and Department of Physics, Bilkent University, Bilkent, 06800 Ankara, Turkey*
[4] *Department of Materials Science and Technology, University of Crete, 71003 Heraklion, Crete, Greece*

(Dated: December 21, 2010)

We experimentally demonstrate, for the first time, an optically-implemented blue-shift tunable metamaterial in the terahertz (THz) regime. The design implies two potential resonance states, and the photo-conductive semiconductor (silicon) settled in the critical region plays the role of intermediary for switching the resonator from mode 1 to mode 2. The observed tuning range of the fabricated device is as high as 26% (from 0.76 THz to 0.96 THz) through optical control to silicon. The realization of broadband blue-shift tunable metamaterial offers opportunities for achieving switchable metamaterials with simultaneous red- and blue-shift tunability and cascade tunable devices. Our experimental approach is compatible with semiconductors technologies and can be used for other applications in the THz regime.

PACS numbers: 78.67.Pt, 78.20.-e, 78.47.-p, 42.25.Bs

The discovery of metamaterials has greatly improved our capabilities in the manipulation of electromagnetic radiation over a large portion of the spectrum [1, 2]. Many intriguing phenomena based on metamaterials, such as superlensing [3, 4] and invisibility [5–8], have been proposed, and studied both theoretically and experimentally. These two ideas (invisibility and superlensing) have attracted the largest research interest recently, but unfortunately, these concepts are hard to be implemented for practical applications. However, terahertz (THz) technology has become a hopeful alternative for sensing, imaging, and applications such as amplifiers, modulators, and switches. One of the greatest obstacles in this progress is the non-existence of materials that naturally respond well to THz radiation. One of the advantages of metamaterials for THz applications is their resonant electromagnetic response, which significantly enhances their interaction with THz radiation. Metamaterials, specifically tailored for the THz regime [9, 10], where response from natural materials is somewhat rare, provide us a more robust up-to-date application of realizing various THz devices to fill the so-called "THz gap" [11–15]. It has been found that hybridized metamaterials, i.e., metamaterials with some external-source-controlled natural materials incorporated, offer us great opportunities in the construction of novel THz devices, such as dynamic notch filters [16–18], phase modulators [19, 20], perfect absorbers [21–23], and frequency-agile switches [24, 25]. In addition, THz radiation has many advantages, such as its non-ionizing property, excellent transmission through optically-opaque materials for imaging applications and the ability to detect biochemical molecules and illegal drugs. So electronic devices are pushing their boundaries to the THz regime, where a lot of potential applications exist in different disciplines.

The key idea is to incorporate photoconductive semiconductors, as elements of metamaterial resonators, and the working frequency of the metamaterial resonator is tuned through photo-excited carrier injections. Chen *et al.* [24] experimentally achieved red-shift tunability, due to a photoconductive increase in the capacitance of the metamaterial resonator. For greater flexibility in practical applications, blue-shift tunable metamaterials are also of great importance and urgent necessity, especially for realizing THz devices simultaneously with red- and blue-shift tunability. However, the achievement of an optical blue-shift switch is really not that easy. Chen *et al.* [24] presented two hypothetical designs targeting this goal, but they were found out of the reach of optical implementation, so they did not demonstrate experimentally the blue-shift. It is found that generally for a simple inductor-capacitor resonator, the optical tuning strategy is easy in realizing an increase of capacitance while may not efficiently change the inductance. In this work, we have designed, fabricated, and characterized the resonant response of a blue-shift tunable metamaterial with photo-excitation, which provide greater flexibility in practical applications. We show that the resonant response can be controlled using optical or electrical approaching, enabling efficient THz switches and modulators, which will be of importance for advancing numerous real world THz applications.

In order to realize a realistic blue-shift tunable metamaterial, a new mechanism of a photo-conductive mode-switching was theoretically proposed [25]. The meta-

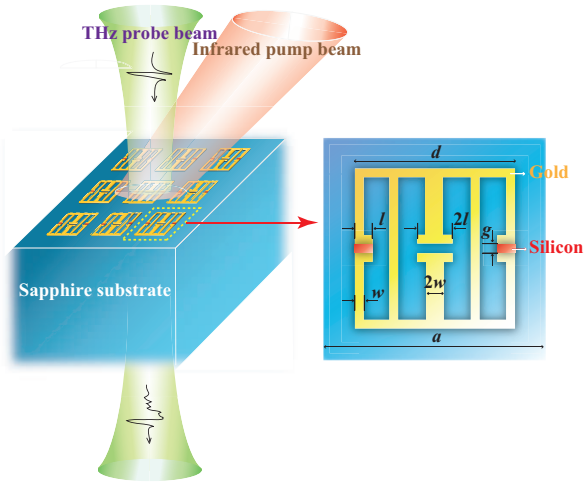

FIG. 1: (Color online) Schematic of our design for broadband blue-shift tunable metamaterial device. Left: Sketch of experimental pump-probe configuration for the measurement of THz transmissions through the fabricated metamaterial device. Right: Top view to the unit cell of the designed structure showing the geometry and dimensions of the device: $a = 50$ μm, $d = 36$ μm, $l = 4$ μm, $w = 2$ μm, and $g = 2$ μm. Photoconductive silicon (red part) is put within two side gaps of the gold ELC resonator (yellow part) and the substrate is made by sapphire (blue part).

material was designed based on electric-field-coupled inductor-capacitor (ELC) resonators [27] and actually evolved from the E1 structure in Ref. 28. The details of the design can be found in Fig. 1, in which photoconductive silicon is put within two side gaps of the metallic ELC resonator in each unit cell. An attentive investigation to the metallic ELC resonator may reveal that it implies two potential resonance states, while the one corresponding to the higher frequency is restrained due to the high intrinsic symmetry of the structure. Compared to the case with no pump, the silicon within the gaps of the two side paths becomes conductive through photoinjection when applying the pump, and the structure is then forced to switch from mode 1 (lower frequency) to mode 2 (higher frequency). In view of an effective circuit model, both inductance and capacitance decrease when the pump is applied, and an all-optical blue-shift switching effect is thereby achieved. Here, we present our experimental demonstration to such a broadband blue-shift tunable metamaterial in the THz regime. This is an important result that gives greater flexibility on multiple switching and modulators using metamaterials, that are tunable to higher (blue-shift) and lower (red-shift) frequencies on photo-excitation.

The metamaterials were fabricated on commercially available silicon-on-sapphire (SOS) wafers, consisting of a 0.6 μm-thick (100) Si epitaxial layer on top of a 530 μm-thick R-plane sapphire substrate. The intrinsic resistivity of the Si epilayer was not measured, but was

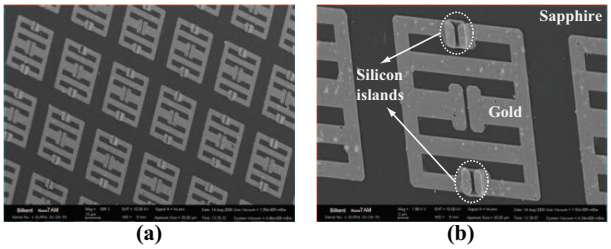

FIG. 2: (Color online) Optical microscopy images of the fabricated metamaterial device. (a) Large area of the device with an array of hybrid metamaterials; (b) Close view of the unit cell.

specified as $>$ 100 Ω cm by the manufacturer. The first step of the fabrication process was the definition of the photosensitive area. This was accomplished by photolithographically protecting the two 6×6 μm^2 regions that coincide with the two side gaps of the metallic resonator, and subsequent reactive ion etching (RIE) of the Si epilayer outside the two side gap regions. Next, the photoresist pattern was removed, and a second RIE step was performed on the entire unprotected sample surface to decrease the thickness of the patterned Si layer from 0.6 to 0.2 μm. This resulted in two $6 \times 6 \times 0.2$ μm mesa-shaped Si photosensitive regions per unit cell. During the last step of fabrication, the metallic resonator pattern aligned to the Si photosensitive mesa was defined by photolithography, 150 Å titanium and 2350 Å gold were deposited by E-beam evaporation. Finally, this is followed by removal of unwanted metal. The fabricated sample for measurement is shown in Fig. 2.

For the experimental study of the metamaterial, a powerful THz time domain spectroscopy (TDS) system has been deployed, using an amplified KHz Ti:Sa laser system delivering 35 fs pulses at 800 nm central wavelength and maximum energy of 2.3 mJ per pulse. Part of the initial laser beam with energy equal to 1.3 mJ was focused in ambient air after partial frequency doubling in a beta-barium-borate crystal (50 mm thick) to produce a two-color filament and subsequently, THz radiation [29, 30].

For the detection of THz radiation, a small fraction of the initial laser pulse probed the THz-induced birefringence in an electro-optic crystal (1 mm-thick ZnTe) and monitored the time profile of the THz electric field. The entire experimental setup was placed inside a purge gas chamber to avoid water vapor absorption of the THz radiation.

To study the dynamic response of the metamaterial, an optical-pump beam (800 nm) was used to excite photocarriers in the silicon. The sample was placed orthogonally on the THz beam path and at the focus of the THz beam, while at 45° to the optical pump beam. At this point, the THz beam spot's diameter measured about 1.2 mm. The temporal delay between the optical pump and the THz beam has been experimentally defined at

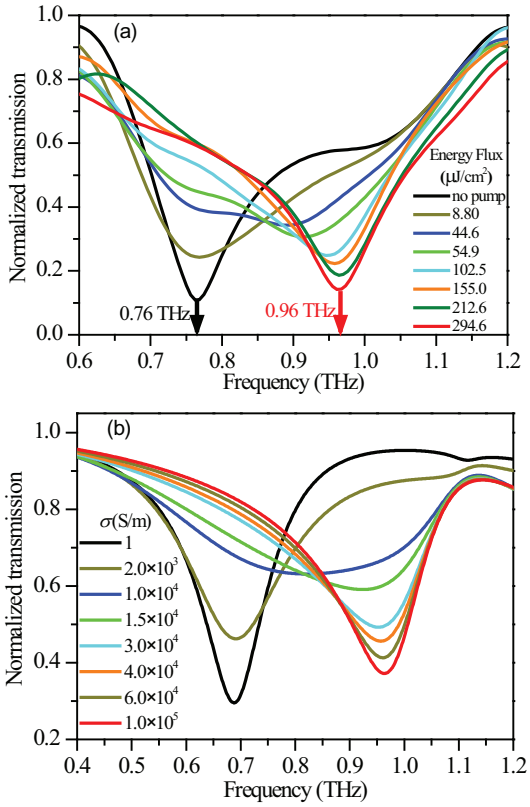

FIG. 3: (Color online) Normalized transmission amplitude of the THz beam for the metamaterial device as shown in Figs. 1-2. (a) Results of experimental measurements as a function of energy flux of pump beam; (b) Results of simulations as a function of conductivity of silicon.

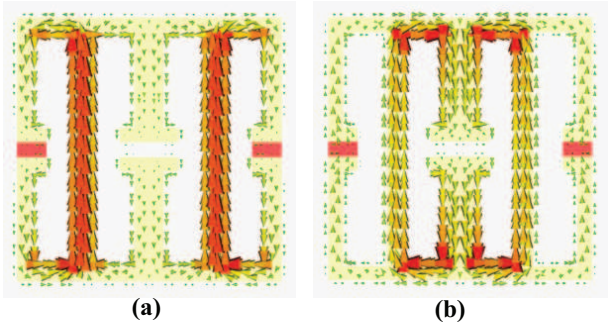

FIG. 4: (Color online) Distribution of surface current density at resonance frequency. (a) Surface current at $f = 0.7$ THz for $\sigma_{\rm Si} = 1$ S/m (case without pump); (b) Surface current at $f = 0.96$ THz for $\sigma_{\rm Si} = 1 \times 10^5$ S/m (case with highest pump intensity). The red parts within the gaps of two side paths are silicon.

around 5 ps (with the photoexcitation occurring before the arrival of the THz beam). This delay assured a quasi-steady state for the charge carriers of silicon since the lifetime (few hundreds of nanoseconds) is orders of magnitude longer than the picoseconds duration of the THz pulse. In addition, to ensure a uniform photo-excitation and the focused optical beam pumps the exact same region of the sample probed by the THz beam, the pump beam was expanded to a diameter of 3 mm and a metallic aperture of 2.2 mm diameter placed immediately in front of the sample. The size of the focused THz beam on the sample was around 2.2 mm. Any residual pump laser radiation, which would bring noise in the detection of the THz electric field, was filtered out by placing a Si wafer (375 mm thick) just after the sample.

The linearly polarized THz electric field is normally incident onto the metamaterial sample or the sapphire substrate, used as reference, and the transmitted THz electric field pulse are coherently recorded in the time domain. The frequency-dependent amplitude $t(\omega)$ of the transmitted THz pulse through the metamaterial is retrieved by the division of the sample spectrum with the reference spectrum $t(\omega) = \mathrm{E}_{\rm sample}(\omega)/\mathrm{E}_{\rm reference}(\omega)$.

The experimental results of the frequency-dependent response of the studied metamaterial are shown in Fig. 3a. With no pump, the normalized transmitted THz electric field amplitude exhibits a minimum of $t(\omega) \approx 10\%$ near the resonance at 0.76 THz (black dashed curve). The off-resonance transmission is around 90%. As the pump energy flux increases, the resonance initially weakens and becomes broader and does not shift in frequency. For cases with a flux value higher than 102.5 μJ/cm^2, the resonance shows a significant shift to higher frequencies. At the level with energy flux 294.6 μJ/cm^2, the resonance dip in the transmission spectrum, $t(\omega) \approx 15\%$, is finally located at 0.96 THz (red line), which corresponds to a fairly broadband blue-shift of 26% in the resonance frequency. Therefore, it is found that the experimental transmission minima for both resonances at 0.76 THz (no pumping) and 0.96 THz (photo-excitation power 294.6 μJ/cm^2) are almost the same. This is a very nice result, which will be ideal to be used for multiple switches and modulators. Our experimental approach is compatible with semiconductor technologies and can be used for other applications in the THz regime.

As a comparison and for understanding our experimental demonstrations, we present in Fig. 3b the results of numerical simulations performed by the commercial software CST Microwave Studio. A single unit cell, as shown in Fig. 1, is adopted for the simulations with appropriate boundaries resembling actual conditions in the THz-TDS experiment. For the metallic parts (gold) of the metamaterial resonator, a lossy-metal model is utilized, the conductivity is $\sigma_{\rm gold} = 7 \times 10^6$ S/m. The sapphire substrate is taken as lossless dielectric with $\varepsilon_{\rm Sapphire} = 10.5$. For the photo-active silicon parts, we applied a simple conductivity model, $\varepsilon_{\rm Si} = 11.7$, and the conductivity, $\sigma_{\rm Si}$, is a pending value chosen to correspond to different pump levels. For the case without illumination, $\sigma_{\rm Si}$was taken to be 1 S/m: the simulated resonance occurs around 0.69

THz and the transmission at resonance is around 30%. Following the increasing pump fluxes, we selected different corresponding values of σ_{Si} to roughly reproduce the experimental results. The final conductivity of Si was taken as high as 1×10^5 S/m only for obtaining similar transmission behavior relative to the no pump case, but it is noticed that actually around $\sigma_{\mathrm{Si}} = 3 \times 10^4$ S/m, the resonance has been shifted close to the final frequency 0.96 THz. Therefore, the simulations showed an all-optical blue-shift with the tuning range of 40%, compared to 26% in the experiments. Despite of some deviation between the simulation and experimental results, which may be mainly due to imperfections in sample preparation, they are overall in quite good agreement with each other. By investigating the distributions of surface current density at two corresponding resonance frequencies for the cases of no pump and highest pump (shown in Fig. 4), we can intuitively understand the underlying physics for our obtained broadband blue-shift tunability: For the case of no pump, the resonator initially works at mode 1 (see the surface current distribution in Fig. 4a) where the two side paths are capacitive, but for the high-pump case, the photo-injection in silicon changes the current distribution (see Fig. 4b) and pushes the structure to work at mode 2 (with higher resonance frequency), where both the effective inductance and capacitance of the structure decrease in the view of a circuit model. Therefore, our blue-shift tunable metamaterial actually works with a photo-excited mode-switching effect, benefiting from the design, which implies two potential resonance states.

In conclusion, we have experimentally demonstrated all-optical broadband blue-shift tunability with a metamaterial design in the terahertz regime. The goal was essentially achieved by our proposed photo-excited mode switching effect, which offers a new path to exploring more designs targeting greater flexibility for practical applications in the range of frequency-agile metamaterials. This work also paves the way for future bi-directional (simultaneously red- and blue-shift) and multi-band even cascade switchable devices, which especially benefits various important THz applications in filling the so-called "THz gap".

Work at Ames Laboratory was supported by the Department of Energy (Basic Energy Sciences) under contract No. DE-AC02-07CH11358. This was partially supported by the European Union Future and Emerging Technologies (FET) project PHOME, and the Marie Curie Excellence Grant "MULTIRAD" MEXT-CT-2006-042683.

* stzortz@iesl.forth.gr
† soukoulis@ameslab.gov

[1] C. M. Soukoulis, S. Linden, and M. Wegener, Science **315**, 47 (2007).
[2] V. M. Shalaev, Nature Photon. **1**, 41 (2007).
[3] J. B. Pendry, Phys. Rev. Lett. **85**, 3966 (2000).
[4] N. Fang, H. Lee, C. Sun, and X. Zhang, Science **308**, 534 (2005).
[5] D. Schurig *et al.*, Science **314**, 977 (2006).
[6] W. Cai, U. K. Chettiar, A. V. Kildishev, and V. M. Shalaev, Nature Photon. **1**, 224 (2007).
[7] J. Valentine, J. Li, T. Zentgraf, G. Bartal, and X. Zhang, Nature Mater. **8**, 568 (2009).
[8] L. H. Gabrielli, J. Cardenas, C. B. Poitras, and M. Lipson, Nature Photon. **3**, 461 (2009).
[9] T. J. Yen *et al.*, Science **303**, 1494 (2004).
[10] A. K. Azad, J. Dai, and W. Zhang, Opt. Lett. **31**, 634 (2006).
[11] B. Ferguson and X. C. Zhang, Nature Mater. **1**, 26 (2002).
[12] R. Köhler *et al.*, Nature **417**, 156 (2002).
[13] R. Kersting, G. Strasser, and K. Unterrainer, Electron. Lett. **36**, 1156 (2000).
[14] K. Wang and D. M. Mittleman, Nature **432**, 376 (2004).
[15] T. Kleine-Ostmann, P. Dawson, K. Pierz, G. Hein, and M. Koch, Appl. Phys. Lett. **84**, 3555 (2004).
[16] H. T. Chen *et al.*, Nature **444**, 597 (2006).
[17] W. J. Padilla, A. J. Taylor, C. Highstrete, M. Lee, and R. D. Averitt, Phys. Rev. Lett. **96**, 107401 (2006).
[18] H. T. Chen *et al.*, Opt. Lett. **32**, 1620 (2007).
[19] H. T. Chen *et al.*, Nature Photon. **3**, 148 (2009).
[20] J. M. Manceau, N. H. Shen, M. Kafesaki, C. M. Soukoulis, and S. Tzortzakis, Appl. Phys. Lett. **96**, 021111 (2010).
[21] N. I. Landy, S. Sajuyigbe, J. J. Mock, D. R. Smith, and W. J. Padilla, Phys. Rev. Lett. **100**, 207402 (2008).
[22] H. Tao *et al.*, Phys. Rev. B **78**, 241103(R) (2008).
[23] B. Wang, T. Koschny, and C. M. Soukoulis, Phys. Rev. B **80**, 033108 (2009).
[24] H. T. Chen *et al.*, Nature Photon. **2**, 295 (2008).
[25] N. H. Shen *et al.*, Phys. Rev. B **79**, 161102(R) (2009).
[26] D. Mittleman, Nature Photon. **2**, 267 (2008).
[27] D. Schurig, J. J. Mock, and D. R. Smith, Appl. Phys. Lett. **88**, 041109 (2006).
[28] W. J. Padilla *et al.*, Phys. Rev. B **75**, 041102(R) (2007).
[29] K. Y. Kim, A. J. Taylor, J. H. Glownia, and G. Rodriguez, Nature Photon. **2**, 605 (2008).
[30] A. Couairon and A. Mysyrowicz, Phys. Rep. **441**, 47 (2007).